Determination of dynamic interfacial tension in a pulsed column under mass transfer condition

Bo Wang[a], Han Zhou[a], Xiong Yu[a], Shan Jing[a], Qiang Zheng[a], Wenjie Lan[b], Shaowei Li[a, *]

[a] *Collaborative Innovation Center of Advanced Nuclear Energy Technology, Institute of Nuclear and New Energy Technology, Tsinghua University, Beijing 100084, China*

[b] *State Key Laboratory of Heavy Oil Processing, China University of Petroleum (Beijing), Beijing 102249, China*

[*] *Corresponding author: lsw@tsinghua.edu.cn Tel: (8610) 80194037 Fax: (8610) 62771740*

Abstract

Interfacial tension is an essential physical property in two-phase flow, and it changes due to the mass transfer. The measurement of dynamic interfacial tension (DIFT) in such a condition is a difficult problem. In the previous study (Zhou et al., Chem Eng Sci. 2019; 197:172-183), we presented the quantitative relation between the droplet breakup frequency function (DBFF) and interfacial tension. It is found that the DBFF is highly depended on interfacial tension. Therefore, the DBFF is a suitable parameter to quantitatively characterize the interfacial tension. Based on this concept, the DIFT in the column is determined by regression method after the DBFF under mass transfer condition is measured. It is found that the DIFT is smaller than the static interfacial tension. This result indicates that interphase mass transfer leads to decreasing of the interfacial tension. The decreasing extent of the DIFT has a positive correlation with the mass transfer flux.

Introduction

Liquid-liquid two-phase flow, a classical but complicated process, is widely used in aromatics extraction, hydrometallurgy, wastewater treatment, nuclear fuel cycle and other processes [1, 2]. In the above processes, production needs are satisfied by different types of equipment such as pulsed column [3], pump-mixer [4], centrifugal contactor [5], micro-fluidic device [6], etc. Among them, the pulsed column is often used in solvent extraction process for it has high mass transfer efficiency [7]. Droplet size is an important parameter affecting mass transfer. It has been found that interfacial tension between the two liquids is a key physical property affecting the droplet size in the pulsed column [8]. In the solvent extraction process, mass transfer between the two fluids occurs, thus the interfacial tension changes dynamically with the process, which is usually referred as dynamic interfacial tension (DIFT). The value of DIFT changes at different location of the pulsed column. Nevertheless, the interfacial tension is usually treated as a constant parameter in most reported works [9-12]. In order to accurately describe the two-phase flow behavior, it is important to quantitatively determine the DIFT in the pulsed column.

As early as the mid-19th century, researchers discovered the Marangoni effect of interfacial liquid flow caused by interfacial tension gradient. By the mid-20th century, Sternling [13] and Maroudas [14] first studied the interfacial instability caused by interfacial mass transfer. In the study of pulsed extraction column, Sawistowski et al. [15, 16] found that the interface area between two liquids was increased due to the instability of the interface under mass transfer conditions. The mass transfer was also strengthened by the convection effect caused by the dynamic interfacial tension. Kleczek et al. [17] found that for some extraction systems, the behavior of

droplets in different regions of the extraction column varies greatly: in some regions, droplets are easily broken into small droplets; in some regions, droplet size is relatively large; in some regions, the degree of droplet sphericity is very high; and in some regions, droplet deformation is serious, even the shape of “liquid filament” and “liquid belt” may be discovered. One of the main reasons for these phenomena is the spatial and temporal distribution of interfacial tension caused by mass transfer, that is, the existence of dynamic interfacial tension. However, these reports have not involved the quantitative characterization of the dynamic interfacial tension. So far, the effect of mass transfer on interfacial tension is rarely considered in the studies on extraction columns [18-21].

In recent years, some researchers have carried out DIFT measurement in microfluidic devices. There are mainly three different categories: (A) The interfacial tension is correlated with the droplet diameter [22-26]. The correlation between interfacial tension and droplet diameter is first determined through a series of experiments. When the interfacial tension changes, the DIFT can be calculated through the correlation once the diameters of droplets are measured. (B) The interfacial tension is calculated by pressure fluctuation [27-29]. In microchannel, pressure fluctuations occur during droplet formation process. The pressure fluctuation was measured by researchers and brought into the Laplace formula to calculate the DIFT. (C) The interfacial tension is calculated by the degree of droplet deformation [30-35]. The deformation of droplets is recorded when they pass through a suddenly enlarged or narrowed microchannel. The interfacial tension in this process can be calculated by using the magnitude of deformation. As a summary, the three DIFT measurement methods based on different principles are developed in the field of microfluids and the measurement is carried out under simple flow conditions. It

is difficult to apply these methods into classical mass transfer equipment because DIFT is strongly depending on the flow field, especially for the equipment with complex flow conditions such as pulsed column. The measuring method for DIFT in such equipment is still not discovered.

Since the DIFT changes with locations in a pulsed column, the main problem to measure the DIFT is to search for a local parameter that is a monotone function of interfacial tension. The traditionally measured parameters, such as holdup and average droplet diameter, do not compliant with this requirement because they are influenced by the upstream or downstream conditions. Comparatively, the droplet breakup frequency function (DBFF), which is defined as the breakup probability of a droplet in unit time, is just such a parameter monotonically related with the interfacial tension. The measurement method for the DBFF in a pulsed disc and doughnut column (PDDC) has been developed in our previous work [36]. This makes it possible to quantitatively characterize the DIFT in the PDDC. Focusing on a location in the PDDC, once the DBFF under mass transfer condition is measured, the DIFT at this location can be determined by regression method. Moving the measuring location one can obtain the spatial distribution of the DIFT. The monotonic relation between the interfacial tension and the DBFF has been provided in our previous study [37].

Based on the above concept, a DIFT measurement method in PDDC under mass transfer condition is developed in this work. To the best of our knowledge, this is the first method to measure the DIFT in the macro-scale two-phase flow. The DITF is measured at different height of the PDDC. Since the mass transfer condition varies with column height, the DITF value is also changed. The main influencing factors that affect DIFT are also discussed. Furthermore,

the breakup behavior under mass transfer condition is investigated and compared to that without mass transfer.

Experiments and methods

Experimental setup

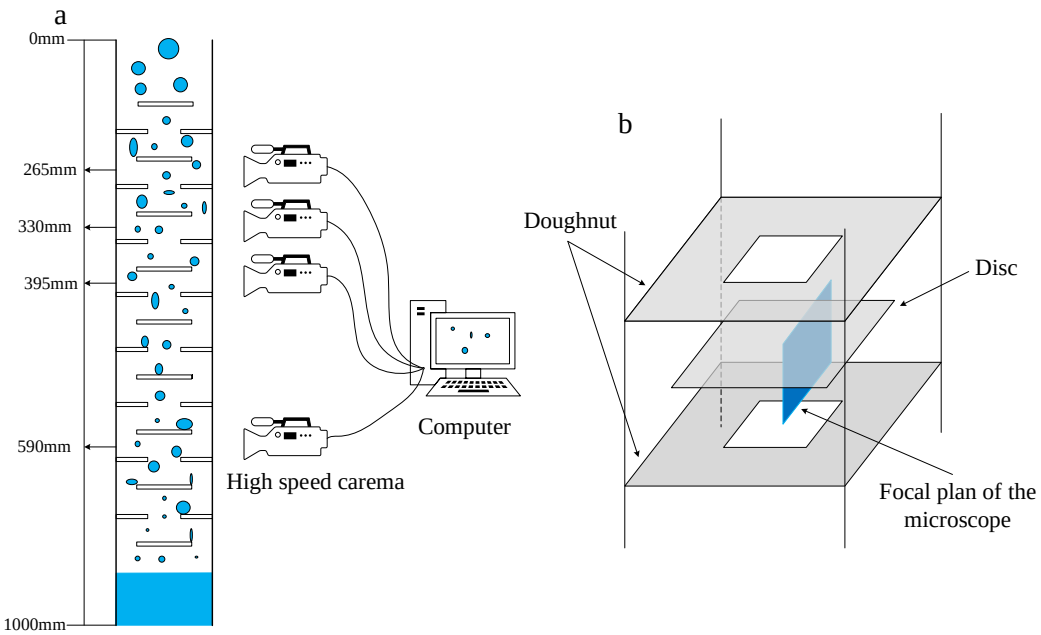

Figure 1. The experimental setup (a) a diagrammatic sketch and (b) in the inner structure of the PDDC.

All experiments were carried out in a laboratory-scale PDDC made of stainless steel. Figure 1 shows the diagrammatic sketch of the experimental set-up. In order to perform a precisely optical measurement, the cross section of PDDC is designed to be square and two glass windows are set on opposite sides of the column. The height of the column is 1000 mm and the dimension of the cross section is 100 mm × 100 mm. Ten pairs of disc and the doughnut plates are arranged alternately in the column. All the plates are made of Teflon with a thickness of 2 mm. The distance between the disc and the doughnut plates is 30 mm. The size of the disc is

87.7 mm × 87.7 mm and the size of the hole in the middle of the doughnut is 48 mm × 48 mm, thus the free area of these two kinds of plates are both 23%. There are seven sampling points arranged equidistantly with an interval of 65 mm along one side of the column. A high-speed camera (Olympus i-Speed TR) connected with a microscope (Olympus SZ61) is used to capture the droplet breakage in the column. The frame rate is 1000 frames per second. The high-speed camera is located at 265 mm, 330 mm, 395 mm and 590 mm from the top of the column respectively, as shown in Figure 1 (a). Figure 1(b) shows the inner structure of the PDDC as well as the focal plane of the microscope connected to the high speed camera. To promote the breakage of droplets in the column, a pulsation generator is connected to the bottom of the column. The pulsation generator induces reciprocal up and down movements of the fluids by a piston, thus a sinusoidal pulsation of the liquid system is produced. The pulsation frequency is 1 Hz and the amplitude is10.5 mm. The aqueous phase entrance and organic phase exit are set at the top of the pulsed column while the aqueous phase exit and organic phase entrance are at the bottom. All exits and entrances are controlled by a supply and collection system respectively. In the process of operation, the aqueous phase is dispersed into droplets in the organic phase by pulsation and the droplets coalesce at the bottom of the column.

Materials

The experiments consist of two parts conclude mass transfer experiments and blank experiments. In mass transfer experiments, 5% (v/v) tributyl phosphate (TBP) in kerosene and 15% (v/v) acetic acid (AC) solution were used as the continuous and dispersed phase separately. The AC, TBP, and kerosene were purchased from Aladdin Reagent Co. Ltd., J&K Scientific

Ltd., and Jinzhou Refinery Factory, respectively. In the blank experiments, 5% (v/v) TBP in kerosene and deionized water were used as the two-phase materials. The physical properties of two-phase materials are shown in Table 1. Continuous phase is pumped into the lower part of the pulsed column by a peristaltic pump (Longer Pump WT600-2J) at the flow rate of 443 mL/min. The dispersed phase is pumped into the upper part of the pulsed column through another peristaltic pump (Longer Pump BT100-2J) at the speed of 21 mL/min. The purpose of choosing a low flow rate of dispersed phase is to reduce the holdup of dispersed phase, so that the behavior of droplets can be optically measured. All experiments were conducted at a temperature of 20±1°C.

Table 1. Physical properties of the two-phase materials used in experiments at 20°C

material	ρ (g/cm3)	μ (mPas)
5% (v/v) TBP in kerosene	0.760	1.69
deionized water	1.002	1.06
15% (v/v) AC solution	1.020	1.10

In all the experiments, the concentrations of AC in both phases were measured by titration method (Metrohm 809 Titrando automatic titrator). The densities were measured by a densitometer (Density Meter DM-340.1, LEMIS Baltic). The viscosities were determined by a viscometer (DV3TLVTJ0, Ametek Brookfield).

Operation procedure

The operation process of mass transfer and blank experiments is basically the same. Firstly,

the continuous phase is filled in the pulsed column. The steady flow of continuous phase can be obtained through continuous phase feed pump. Then, the pulsation generator is turned on at the time that the dispersed phase is added. After a periodical steady state is achieved (the AC concentration does not change for both the discharged continuous and dispersed phases), the high-speed camera is turned on to record the droplet behavior at different heights of the column. At each location, the high-speed camera records totally 97.88 seconds (97,880 images). The droplet diameter is measured by GetData software and the droplet number density is counted at the same time. Droplet breakage is counted manually. During the experiment, the measurement errors caused by different refractive index can be eliminated by calibrating a standard length of pixel size.

Method

The measurement of DIFT in the PDDC is divided into three steps. Firstly, the number density functions of droplets at different heights are measured. Then the DBFF is determined based on the obtained number density function after the droplet breakup events are counted. Finally, the obtained DBFF is submitted into the correlation between the interfacial tension and DBFF for regression, in order to determine the value of DIFT. The detailed description for the three steps is as follows.

The droplet number density function is denoted as $n(D)$. $n(D)\mathrm{d}D$ is defined as the number of droplets within the infinitesimal size interval of dD about size D per unit volume. Thus $n(D)$ has a unit of (m^{-4}). In order to measure $n(D)$, the differential dD is replaced by difference ΔD, and $n(D)$ can be calculated by Eq. 1.

$$n(D)\Delta D = \frac{N(D)}{V} \tag{1}$$

In Eq.1, $N(D)$ is the counted number of droplets within size interval ΔD about size D. V is the volume used for counting the droplet number.

The DBFF is defined as the breakup probability of a droplet in unit time. It has another equivalent definition, the breakup proportion of droplets per unit time. It can be determined based on Eq. 2 which is also used by Zhou [36, 37].

$$\Gamma(D) = \frac{1}{t_c}\left(\frac{\text{number of droplet breakup events}}{\text{number of droplets}}\right) = \frac{1}{t_c}\frac{n_b(D)\Delta D}{n(D)\Delta D} \tag{2}$$

In Eq.2, $n_b(D)\Delta D$ represents the number of breakup events within time t_c in unit volume for droplets within size interval from $(D-\Delta D/2)$ to $(D+\Delta D/2)$. t_c represents the duration of the measurement. The droplet diameter D is determined by $D=(ab)^{1/2}$ in the 2D images after measuring the long axis *a* and short axis *b* of the droplet. After $n_b(D)\Delta D$ and $n(D)\Delta D$ are counted from the video captured by the high speed camera, DBFF can be determined.

The DBFF obtained above is then applied to determine the value of DIFT by regression method based on Eq. 3, which was established in our previous work based on systematical experiments [37]. The value of DIFT changes with the column height since the DBFF measured at every height is different, because the mass transfer condition varies along the column.

$$\Gamma(D) = 1.825\times10^{6}\frac{Af}{H}\left(\frac{AfD\rho_c}{\mu_d}\right)^{0.0452}\left(\frac{(Af)^2 D\rho_c}{\gamma}\right)^{3.2598} \tag{3}$$

In Eq. 3, A represents the pulsation amplitude. f is pulsation frequency. H represents the plate spacing. ρ_c and μ_d represent continuous phase density and dispersed phase viscosity, respectively. γ is the interfacial tension or DIFT in mass transfer conditions. It

should be noticed that the DIFT determined by this method is an equivalent average interfacial tension on a cross section of the column. The variation of DIFT in the cross section is not considered.

Results and discussion

Determination of dynamic interfacial tension

Number density function

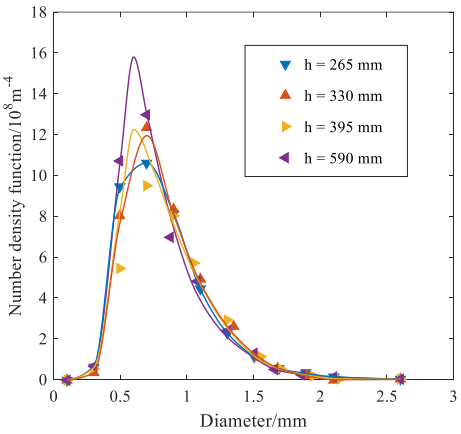

Figure 2. Number density of the droplets for different height.

According to Eq. 1, the droplet number density function $n(D)\Delta D$ should be obtained before determining the DBFF. The droplet number density function at different height is shown in Figure 2. It can be seen that the droplet size shows a positive skewed distribution at different column height. This is different from the results in our previous report [36, 37] where the droplet size showed a normal distribution. The reason is probably the introduced mass transfer changed the behaviors of droplets. It is also found that the droplet diameter mainly distributes between 0.3 mm and 1.8 mm. The number density of droplets smaller than 0.3 mm is small because it is difficult for large droplets to produce such small daughter droplets (heterogeneous breakup)

in the process of breaking up. The surface energy of small droplets is large, the energy consumed in the process of droplet breaking is insufficient to support the formation of such small droplets under the energy inputting condition in our experiments. The number density of droplets lager than 1.8 mm is small because the breakup of large droplets is easier. The breakup frequency for droplet larger than 1.8 mm is much larger in this work, which will be shown in the next section. It can be further seen that the number density of small droplets (around 0.75 mm) increases with the increasing of column height. The reason is that the droplets from upstream are further broken up when they go downstream and therefore the number of small droplets increases.

Experimental result on drop breakup frequency function

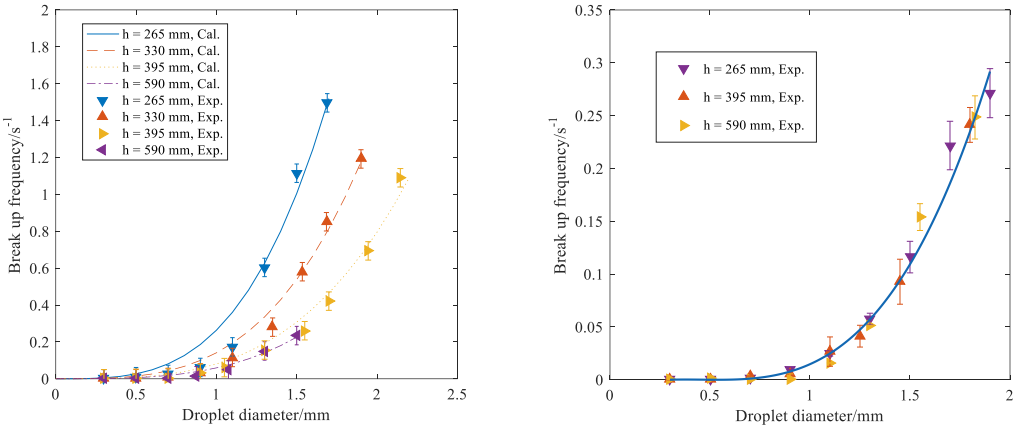

(a) (b)

Figure 3. Statistical results of DBFF. (a) The DBFF at different height under mass transfer condition. (b) The DBFF at different height for the blank experiments without mass transfer.

In above Section, the droplet number density functions at different height have been obtained.

The breakup frequency functions at different heights of the column can then be determined through the method described in experiments and methods. The results are shown in Figure 3(a). In turbulent flow field, large droplets receive more energy due to the collision of more turbulent eddies and are more likely to break up. Figure 3(a) also shows that the DBFFs for droplets with the same diameter are different at different heights. The DBFF is the highest at 265 mm and then decreases gradually with the increasing of column height. In our experiment, the operating conditions of the extraction column are unchanged, so the turbulent kinetic energy along the column height should be the same. For droplets of the same size, the frequency of turbulent eddy collision is also the same. In this scenario, the breakup frequency changing at different height is mainly caused by the variation of interfacial tension. In the extraction column, the concentrations of solute in the two phases change with the column height while the existence of mass transfer process also causes the instability of the interface. These two aspects will ultimately affect the interfacial tension. The interfacial tension at different height can then be determined by regression from the measured breakup frequency. In this way, the DIFT in the pulsed column can be measured.

As a comparison, blank experiments are carried out in order to confirm that the breakup frequency is not affected by the column height without mass transfer. Deionized water and 5% (v/v) TBP in kerosene are used as the dispersed and continuous phase separately. By using the same statistical method as mass transfer experiments, the DBFFs at different height are measured. The results are shown in Figure 3(b). We can see from the figure that the DBFFs at different height are almost the same in the blank experiments without mass transfer. This result further proves that the DBFF curves shown in Figure 3(a) have a one - to - one correspondence

with the DIFT in the pulsed column.

Regression of dynamic interfacial tension

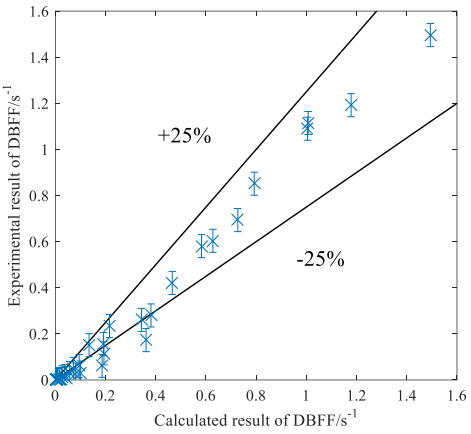

Figure 4. Comparison of the result of DBFF between the experiment and calculation based on the regressed DIFT.

We have presented in the above section that the DBFF changes monotonically with DIFT. To determine DIFT, the quantitative relationship between the DBFF and the interfacial tension is required. We have presented such a correlation between the DBFF and the static interfacial tension in our previous research [37], as shown in Eq. 3. This equation provides a bridge between the DIFT and the static interfacial tension, helps us quantitatively characterize the DIFT with a serials of known static interfacial tension.

Based on the experimental data in Figure 3(a), the interfacial tension γ in Eq. 3 was regressed by nonlinear least square fitting. The obtained values of DIFT at different height are shown in Table 2. With these DIFT, the calculated DBFFs are shown in Figure 3(a) as curves. Figure 4 also shows the comparison between the calculated results and the experimental results for DBFF. Considering that there is an error of about 0.05 s^{-1} in the statistical process [36, 37],

the experimental results below 0.1 s^{-1} are useless for evaluating the calculated results. We can see from Figure 4 that the prediction error of this correlation is within ±25% when the DBFF is greater than 0.1 s^{-1}. The correlation in our previous work with different static interfacial tensions fits well with the experimental data of this work with DIFTs.

As a comparison, the static interfacial tension was also regressed from the DBFFs measured in the blank experiments. The results were also listed in Table 2. We can see that the obtained interfacial tensions are almost the same at different height of the column. Furthermore, the result is approximately equal to that measured by pendent drop method (14.98 mN/m). These results furtherly proved the feasibility of the regression method. Moreover, we can see from Table 2 that the DIFT increases from the column top to bottom, and almost reaches the value of equilibrium interfacial tension (12.8 mN/m, measured by pendent drop method) at the height of 590 mm. The variation of DIFT along the column will be discussed in detail in the next section.

Table 2. The regressed interfacial tension in different height

Height (mm)	DIFT *(mN/m)	Static interfacial tension **(mN/m)
265	7.82	14.78
330	9.47	-
395	11.25	14.99
590	12.55	14.82

* regressed from the DBFFs measured in mass transfer experiments

** regressed from the DBFFs measured in blank experiments

Analysis of influencing factors of DIFT

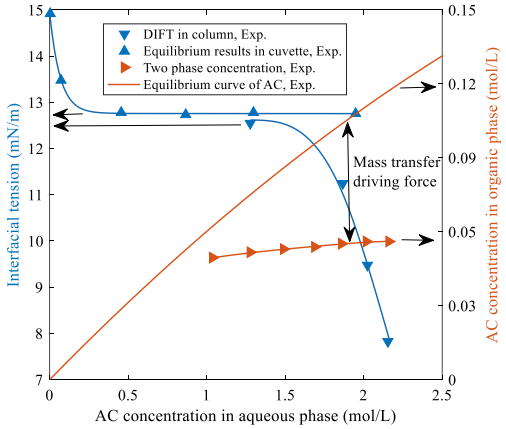

Figure 5. The relationship between interfacial tension and concentration of two phases.

We have shown that the DIFT varies with the column height in the above text. However, it is still an important issue to analyze the intrinsic influencing factors of DIFT. Comparing to the blank experiments, AC is introduced into the system under mass transfer conditions and the concentration of AC will affect the interfacial tension. In addition, due to the interphase mass transfer, the interface between the two phases will be disturbed (partially attributed to the well-known Marangoni effect), resulting in change of interfacial tension. Preliminary analysis shows that the above two factors are responsible for the dynamic change of interfacial tension under mass transfer conditions. To analyze the contribution of these two factors, the AC concentration profile in the column needs to be measured.

Because of the low fraction of dispersed phase in this experiment, only continuous phase can be led off from the sampling port of the column. The AC concentrations in the continuous phase from different sampling points are measured by titration and the results are shown in Table 3. Though the AC concentration profile of dispersed phase cannot be directly measured,

it can be calculated based on the concentration profile of continuous phase through the axial diffusion model [38]. The calculation AC concentration profile in dispersed phase is shown in Table 3. The calculated process is described in the Appendix. We can see that the calculated AC concentration in the dispersed phase at the bottom of the column is 1.04 mol/L, which is almost equal to the measured AC concentration at the aqueous phase outlet (1.05±0.03 mol/L). This result proves that the calculated AC concentration in the dispersed phase by axial diffusion model is trustable.

Table 3. The concentration in different heights of the continuous phase and dispersed phase.

Height (mm)	Concentration of AC in the continuous phase (mmol/L)	Calculated concentration of AC in the dispersed phase (mol/L)
5(outlet)	56.10±0.03	-
265	56.05±0.03	2.16
330	55.85±0.03	2.02
395	54.97±0.03	1.86
460	54.05±0.03	1.69
525	52.85±0.03	1.49
590	51.50±0.03	1.28
655	49.47±0.03	1.04
inlet	2.64±0.03	-

To analyze the DIFT influencing factors, the AC concentration in both liquids as well as the

DIFT are displayed together as shown in Figure 5. As a comparison, the static interfacial tension for two phases in equilibrium state is also displayed in the figure. The static interfacial tension was measured by pendent drop method (LSA100 Surface Analyzer, LAUDA).

It can be found from Figure 5 that the static interfacial tension between the two phases decreases with the increase of the AC concentration (in both phases) under equilibrium conditions. When the concentration of AC continues to increase, the static interfacial tension between the two phases reaches a platform when the AC concentration in aqueous phase (C_a) is higher than a critical point. The critical point of C_a is approximately 0.3 mol/L. However, under mass transfer conditions in the column, the dynamic interfacial tension between the two phases decreases continuously with the increase of aqueous phase concentration. Comparing these two curves, we can derive that the effect of concentration change on dynamic interfacial tension has been pretty weak because the concentration in the column is much higher than the critical point. Therefore, the main reason for the decrease of dynamic interfacial tension is the disturbing effect of mass transfer.

In order to further analyze the relationship between dynamic interfacial tension and mass transfer, the equilibrium relation of AC in both phases was measured and displayed in Figure 5 as the equilibrium line. The AC concentrations of both phases in the column are displayed as the operation line in Figure 5. The concentration difference between the equilibrium line and the operating line is the mass transfer driving force. It can be clearly seen that the larger the mass transfer driving force is the larger the difference between DIFT and static interfacial tension is. Larger driving force leads to higher mass transfer rate. Thus, the above results illustrate that the dynamic interfacial tension decreases with the increasing of mass transfer rate,

probably due to the disturbing effect of mass transfer on the interface.

To quantitatively analyze the effect of the mass transfer rate on the DIFT, the mass transfer flux at different height of the column is calculated based on mass conservation. The calculating result is shown in Figure 6. Though an empirical correlation equation cannot be established due to the small number of data points, the results provides the first quantitative relation between the mass transfer flux and the DIFT. A method to quantitatively study the DIFT in columns is proposed.

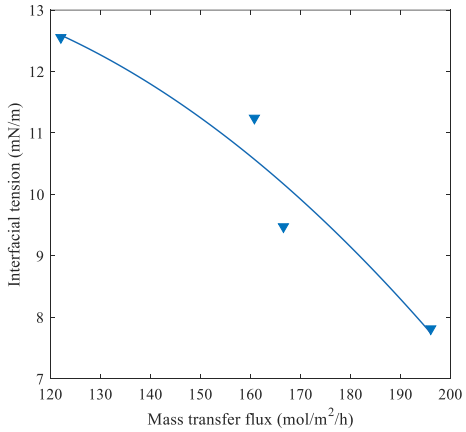

Figure 6. The relationship between mass transfer flux and interfacial tension.

Droplet breakup behavior under mass transfer condition

Under mass transfer conditions two types of droplet breakage patterns, tensile breakup and revolving breakup, was observed as shown in Figure 7. This phenomenon is the same with that in our previous work without mass transfer [36]. We can then conclude that the breakup pattern is little affected by mass transfer in the PDDC within our experimental conditions.

The fragment number of droplets is also a research contents in addition to the breakup patterns of droplets. As shown in Figure 8 (a), droplet breakup can be found at different heights from binary breakup to quintuple breakup under mass transfer conditions. Among these results,

the binary breakup ratio occupies the main position. In the process of droplet breaking, the energy required for binary breaking is the lowest, so its breaking standard is easy to achieve. With the increase of the number of droplets produced by breaking, the energy required will increase.

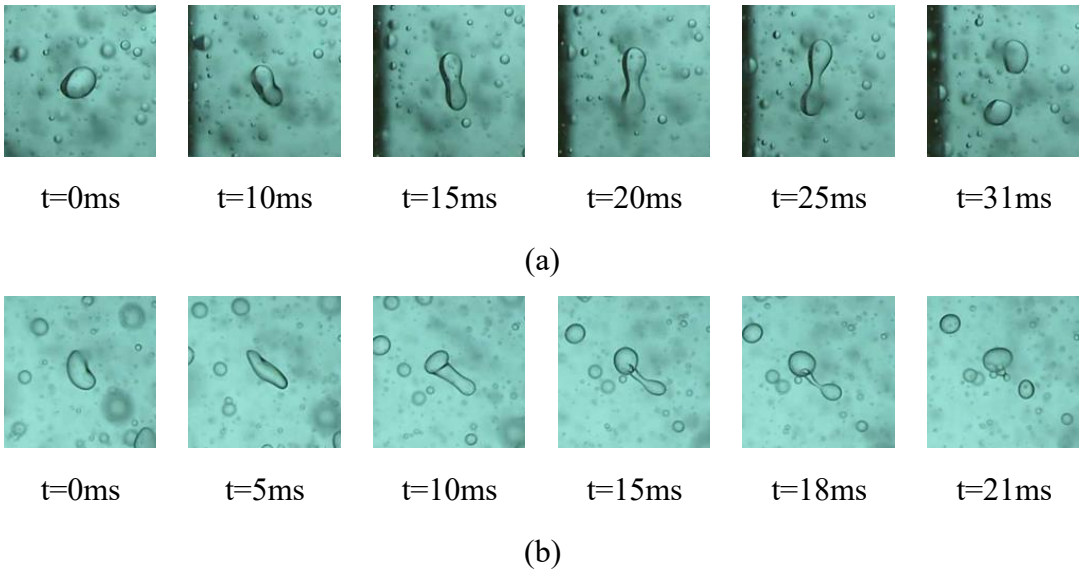

Figure 7. The main droplet breakup patterns (a) Tensile breakup. (b) Revolving breakup.

We can further see from Figure 8 (a) that, at the height of 265 mm, the proportion of binary breakage is the lowest, while that of multiple breakage is the highest. According to the calculation results, the reason may be that the interfacial tension at this location is small and the energy required for droplet breakup in small interfacial tension system is less. In the same turbulent flow field, multiple breakup is more likely to occur, which results in the lowest proportion of binary breakup of droplets at the height of 265 mm. The influencing trend of DIFT on the ratio of different number of breakage is the same with that of different values of static interfacial tension presented in our previous work [37]. This proves that the DIFT in this

work is a proper defined parameter characterizing the effect of mass transfer.

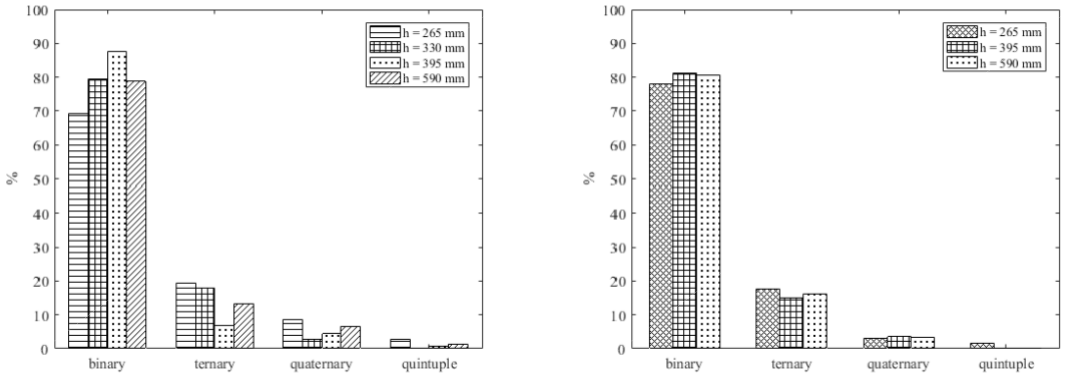

(a) (b)

Figure 8. The relative appearance between binary, ternary, quaternary and quintuple breakage in different height (a) under mass transfer condition and (b) without mass transfer condition.

Figure 8(b) shows the proportion of droplet breakage at different heights without mass transfer. It can be seen from the figure that, unlike mass transfer conditions, at different heights, the proportion of binary, ternary and quaternary breakage of droplets is almost the same. In the height of 265 mm, a small amount of quintuple breakage occurs. However, no quintuple fragmentation is found at other heights. Under no mass transfer condition, the interfacial tension between the two phases does not change with the height, thus the ratio of fragmentation tends to be the same.

Figure 9 shows that the proportion of binary breakup is different under various mother droplet diameters. When the droplet diameter is small, the proportion of binary breakup at different heights is higher than 85%. With the increase of the diameter of mother droplets, the proportion of binary breakage decreases gradually. With the increase of the diameter of mother

droplets, the instability of the interface will increase, which will increase the probability of multiple fragmentation. In addition, in the turbulent flow field, droplets with larger diameter are also vulnerable to more turbulent eddy collisions, thus obtaining more energy and undergoing multiple breakup.

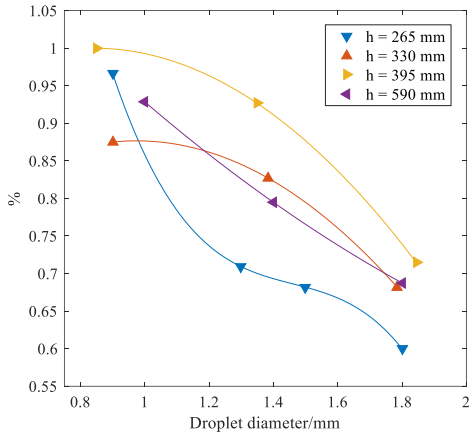

Figure 9. The proportion of binary breakage in different height and different diameter of mother droplets under mass transfer condition.

Daughter droplet size distribution

The DDSD is also an important parameter in the process of droplet breakup. It directly reflects the diameter of daughter droplets generated after droplet breakup and also reveals whether the droplet breaks equally or unevenly in the system. The multiple breakage is treated as a series of binary breakage with the method reported in our previous work [36]. Figure 10 shows the experimental results of DDSD at different height. The results show that the DDSD is inverted U-shaped under mass transfer conditions. At the same time, the size distribution of daughter droplets produced by breaking mother droplets with different diameters is similar. The reason may be that under mass transfer conditions, the droplet diameter in the experimental

system is relatively small and these droplets are more prone to tensile breakage. The small droplets produced in the process of tensile breakage tend to be equal in diameter. Therefore, the DDSD shows an inverted U-shaped distribution.

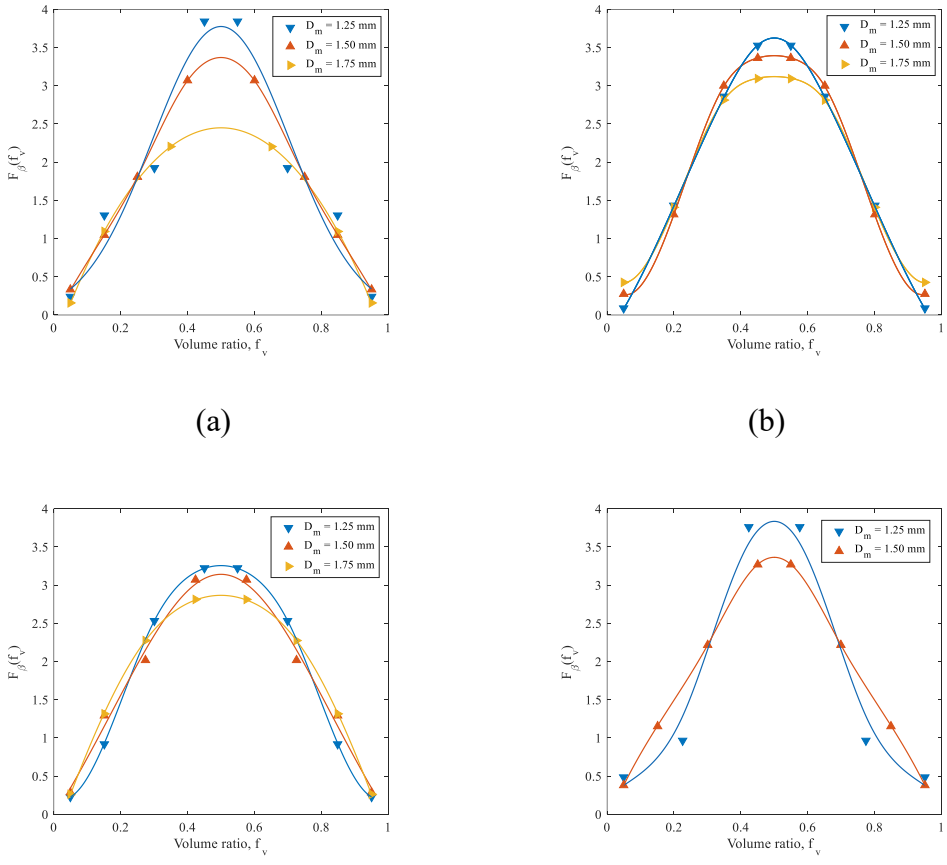

Figure 10. Experimental results of DDSD in different height. (a) *h* = 265 mm. (b) *h* = 330 mm. (c) *h* = 395 mm. (d) *h* = 590 mm.

The experimental results were compared with the predicted results by the DDSD model in our previous work [37] as shown in Figure 11. The comparing method was described in detail in that work. It was found that the predicted results were within an error of ±25% when the measured DIFT were introduced into the equation. It is shown that the correlations for breakup

frequency and DDSD obtained under the conditions without mass transfer in our previous work [37] can be directly applied to the prediction of droplet behavior in mass transfer process after the DIFT is determined. This also proves that to introduce a single parameter of DIFT is sufficient to describe the droplet breakage under mass transfer conditions in the PDDC, no other parameters are needed.

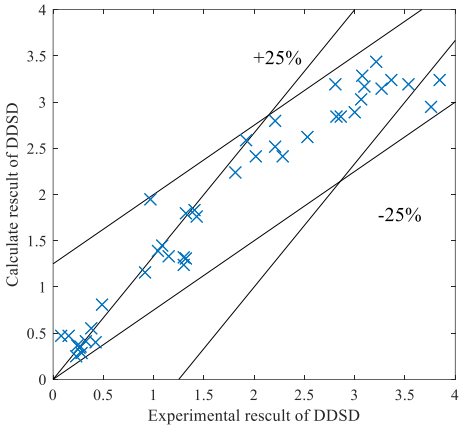

Figure 11. Comparison between the experimental results of DDSD and that calculated by our previous correlation [37].

Conclusions

In this work, a method to quantitatively characterize the DIFT in PDDC is developed based on the measurement of DBFF. We found that the DBFF varies with column height in the PDDC under mass transfer conditions. This variation is attributed to the interfacial tension changing caused by mass transfer. The changing interfacial tension along the height of the PDDC is defined as DIFT. A correlation between the DBFF and the static interfacial tension obtained under conditions without mass transfer in our previous work was used to determine the DIFT. The values of DIFT along the column height were obtained by regressing the interfacial tension in the correlation. By analyzing the equilibrium interfacial tension and DIFT between two

phases, it was found that the difference between the DIFT and the equilibrium interfacial tension has a positive correlation with the mass transfer flux. Moreover, it is found that there are two types of breakage patterns, ensile breakup and revolving breakup, under mass transfer conditions. Binary breakup plays a dominant role in droplet breakup events at different height of the column. Under mass transfer conditions, the DDSD is inverted U-shaped at different heights. To introduce a single parameter of DIFT is sufficient to describe the droplet breakage under mass transfer conditions in the PDDC, no other parameters are needed.

Acknowledgments

We gratefully acknowledge the support of the National Natural Science Foundation of China (21776151, 21576147, 21376132).

Notation

Latin symbols

$n(D)$ droplet number density, m^{-4}

$N(D)$ number of droplets with diameter D

D droplet diameter, mm

V volume, m^3

t_c duration of the fragmentation event, s

ΔD diameter interval, mm

a long axis of droplet, mm

b short axis of droplet, mm

F_β daughter droplet size distribution function

D_m diameter of mother droplet, mm

f_v volume ratio of the droplet to the mother droplet

f pulsation frequency, s-1

A pulsation amplitude, mm

H Height of half unit, m

V_a the flow rate of dispersed phase, m/s

V_o the flow rate of continuous phase, m/s

C_a the concentration of dispersed phase, mol/L

C_o the concentration of continuous phase, mol/L

h height, mm

E_c the axial mixing coefficient

H^* distance between sampling points, mm

t time, s

Greek letter

ρ density, g/cm3

μ viscosity, mPas

$\Gamma(D)$ droplet breakup frequency function, s-1

ρ_c continuous phase density, kg m-3

μ_d viscosity of the dispersed phase, Pa s

γ interfacial tension, mN/m

Abbreviations

DIFT dynamic interfacial tension

DBFF droplet breakup frequency function

PDDC pulsed disc and doughnut column

TBP tributyl phosphate

AC acetic acid

2D two-dimensional

DDSD daughter droplet size distribution

References

1. Fletcher JM. Solvent extraction chemistry. *Nature*. 1963; 197(4871):957-958.
2. Rosenbaum JB. Minerals extraction and processing: new developments. *Science*. 1976; 191(4228):720-723.
3. Yi H, Wang Y, Smith KH, Fei WY, Stevens GW. Hydrodynamic performance of a pulsed solvent extraction column with novel ceramic internals: holdup and drop size. *Ind Eng Chem Res.* 2017; 56(4): 999-1007.
4. Zhou H, Yu X, Jing S, Zhou H, Lan WJ, Li SW. Measurement of droplet breakage in a pump-mixer. *Chem Eng Sci.* 2019; 195:23-28.
5. Wyatt NB, O'Hern TJ, Shelden B. Drop size distributions and spatial distributions in an annular centrifugal contactor. *AIChE J.* 2013; 59(6):2219-2226.
6. Xu JH, Li SW, Tan J, Wang YJ, Luo GS. Preparation of highly monodisperse droplet in a T-junction microfluidic device. *AIChE J.* 2006; 52(9):3005-3010.
7. Wang Y, Mumford KA, Smith KH, Li Z, Stevens GW. Dispersed-phase holdup and characteristic velocity in a pulsed and nonpulsed disk-and-doughnut solvent extraction column. *Ind Eng Chem Res.* 2016; 55(3):714-721.

8. Liu JQ, Li SW, Jing S. Hydraulic performance of an annular pulsed disc-and-doughnut column. *Solvent Extr Ion Exc.* 2015; 33(4):385-406.
9. Kumar A, Hartland S. A unified correlation for the prediction of dispersed phase hold-up in liquid-liquid extraction equipment. *Ind Eng Chem Res.* 1995; 34(11):3925-3940.
10. Kumar A, Hartland S. Prediction of drop size in pulsed perforated-plate extraction columns. *Chem Eng Commun.* 1986; 44(1-6):163-182.
11. Coulaloglou CA, Tavlarides LL. Description of interaction processes in agitated liquid-liquid dispersions. *Chem Eng Sci.* 1977; 32:1289-1297.
12. Luo H, Svendsen HF. Theoretical model for drop and bubble breakup in turbulent dispersions. *AIChE J.* 1996; 42(5):1225-1233.
13. Sternling CV, Scriven LE. Interfacial turbulence: hydrodynamic instability and the Marangoni effect. *AIChE J.* 1959; 5(4):514-523.
14. Maroudas NG, Sawistowski H. Surface renewal and molecular diffusion in interphase mass transfer. *Nature.* 1960; 188(4757):1186-1187.
15. Sawistowski H. Influence of mass-transfer-induced Marangoni effects on magnitude of interfacial area and equipment performance in mass transfer operations. *Chem Ing Tech.* 1973; 45(18):1114-1117.
16. Sawistowski H. Surface-tension-induced interfacial convection and its effect on rates of mass transfer. *Chem Ing Tech.* 1973; 45(18):1093-1098.
17. Kleczek F, Cauwenberge V, Rompay PV. Effect of mass transfer on droplet size in liquid-liquid dispersions. *Chem Eng Technol.* 1989; 12(1):395-399.
18. Lade VG, Pakhare AD, Rathod VK. Mass transfer studies in pulsed sieve plate extraction column for the removal of tributyl phosphate from aqueous nitric acid. *Ind Eng Chem Res.* 2014; 53(12):4812-4820.
19. Wang Y, Yi H, Smith KH, Mumford KA, Stevens GW. Mass transfer in a pulsed and non-pulsed disc and doughnut (PDD) solvent extraction column. *Chem Eng Sci.* 2017; 165:48-54.
20. Yi H, Wang Y, Smith KH, Fei WY, Stevens GW. Axial dispersion and mass transfer of a pulsed solvent extraction column with novel ceramic internals. *Ind Eng Chem Res.* 2017; 56(11):3049-3058.
21. Liu JQ, Li SW, Jing S. Axial mixing and mass transfer performance of an annular pulsed disc-and-doughnut column. *Solvent Extr Ion Exc.* 2015, 33(6):592-606.
22. Xu JH, Li SW, Lan WJ, Luo GS. Microfluidic approach for rapid interfacial tension measurement. *Langmuir.* 2008; 24(19):11287-11292.

23. Wang K, Lu YC, Xu JH, Luo GS. Determination of dynamic interfacial tension and its effect on droplet formation in the T-shaped microdispersion process. *Langmuir.* 2009; 25(4):2153-2158.
24. Steegmans MLJ, Warmerdam A, Schroën KGPH, Boom RM. Dynamic interfacial tension measurements with microfluidic Y-junctions. *Langmuir.* 2009; 25(17):9751-9758.
25. Dong PF, Xu JH, Zhao H, Luo GS. Preparation of 10μm scale monodispersed particles by jetting flow in coaxial microfluidic devices. *Chem Eng J.* 2013; 214:106-111.
26. Nguyen NT, Lassemono S, Chollet FA, Yang C. Interfacial tension measurement with an optofluidic sensor. *IEEE Sens J.* 2007; 7(5):692-697.
27. Wang X, Riaud A, Wang K, Luo GS. Pressure drop-based determination of dynamic interfacial tension of droplet generation process in T-junction microchannel. *Microfluid Nanofluid.* 2015; 18(3):503-512.
28. Lan WJ, Wang C, Guo XQ, Li SW, Luo GS. Study on the transient interfacial tension in a microfluidic droplet formation coupling interphase mass transfer process. *AIChE J.* 2016; 62(7):2542-2549.
29. Lan WJ, Wang ZH, Wang M, Liu D, Guo XQ, Sun Q, Li XX, Li SW. Determination of transient interfacial tension in a microfluidic device using a laplace sensor. *Chem Eng Sci.* 2019; 209:1-9.
30. Brosseau Q, Vrignon J, Baret J. Microfluidic dynamic interfacial tensiometry(μDIT). *Soft Matter.* 2014; 10:3066–3076.
31. Glawdel T, Ren CL. Droplet formation in microfluidic T-junction generators operating in the transitional regime. III. Dynamic surfactant effects. *Phys Rev E.* 2012; 86(2):026308.
32. Glawdel T, Elbuken C, Ren CL. Droplet formation in microfluidic T-junction generators operating in the transitional regime. I. Experimental observations. *Phys Rev E.* 2012; 85(1-2): 026308.
33. Glawdel T, Elbuken C, Ren CL. Droplet formation in microfluidic T-junction generators operating in the transitional regime. II. Modeling. *Phys Rev E.* 85(1-2):016323.
34. Cabral JT, Hudson SD. Microfluidic approach for rapid multicomponent interfacial tensiometry. *Lab Chip.* 2006, 6(3):427-436.
35. Martin JD, Marhefka JN, Migler KB, Hudson SD. Interfacial rheology through microfluidics. *Adv Mater.* 2011, 23(3):426-432.
36. Zhou H, Jing S, Fang Q, Li S, Lan WJ. Direct measurement of droplet breakage in a pulsed disc and doughnut column. *AIChE J.* 2017; 63(9):4188-4200.
37. Zhou H, Jing S, Yu X, Zhou H, Lan WJ, Li SW. Study of droplet breakage in a pulsed disc and doughnut column-Part I: Experiments and correlations. *Chem Eng Sci.* 2019; 197:172-183.

38. Wang Y, Yi H, Smith KH, Mumford KA, Stevens GW. Axial dispersion in a pulsed and nonpulsed disc and doughnut solvent extraction column. *Ind Eng Chem Res.* 2017; 56(14):4052-4059.